ECTI Transactions on Computer and Information Technology
Journal homepage: https://ph01.tci-thaijo.org/index.php/ecticit/
Published by the ECTI Association, Thailand, ISSN: 2286-9131

Glaucoma Detection Based on Specularity Removal Low Rank Model from Retinal Fundus Images

Satyabrata Lenka[1], Mayaluri Zefree Lazarus[2] and Saubhagya Ranjan Behera[3]

ABSTRACT

Glaucoma is one of the eye diseases that affect the optic nerves which connect the eye to the human brain. Detection of glaucoma; in the early stages prevents loss of vision. Automatic detection of glaucoma; becomes a technical challenge for image processing using convex approximation. Fundus images of the eye are taken by a fundus camera through which automatic detection is possible. The retinal fundus imaging process suffers from nonuniform illumination problems due to the curved surface of the retina and pupil dilation, which affects glaucoma detection. The prime objective of this research is to provide the best low-rank model for specularity removal from the retinal fundus images using the Robust PCA algorithm for better screening without losing important information. The Cup to Disc Ratio (CDR) in the fundus image is calculated from Optic Disc (OD) and Optic Cup (OC) segmentation and Support Vector Machine (SVM), a machine learning algorithm mostly popular for binary classification. We use ORIGA, Drishti-GS-RETINA, and REFUGE databases of fundus images for the experimental analysis and MATLAB implementation. The paper presents a comparison of five RPCA algorithms, and the success rate of glaucoma detection increases to 97% using the IALM method. The proposed method provides a pre-processing step for specularity removal from fundus images and improves the glaucoma detection rate.

Article information:

Keywords: Glaucoma Detection, Fundus Image, Feature Extraction, Specularities, Glare Removal

Article history:
Received: December 19, 2022
Revised: April 8, 2023
Accepted: July 3, 2023
Published: July 22, 2023
(Online)

DOI: 10.37936/ecti-cit.2023173.251084

1. INTRODUCTION

Glaucoma is an ophthalmic disease that causes blindness, and the loss of vision due to glaucoma cannot be reversed. Approximately 111.8 million people may suffer from glaucoma by the end of the year 2040 [1]. A fluid named aqueous humor is filled in the frontal portion of the human eye, which maintains a stable pressure called intraocular pressure (IOP). There is a continuous process of fluid formation and drain out to maintain a stable pressure inside the eye. Glaucoma typically arises when the fluid inside the eye does not drain out. The aqueous humor fluid gradually builds up, increases pressure inside the eye, and damages the optic nerve, which is mainly in control of sending visual messages in the form of electrical signals from the human eye to the brain. Many people are oblivious to their condition because it has no early symptoms. The capacity of human vision loss due to glaucoma diseases can often be prevented with early screening and diagnosis.

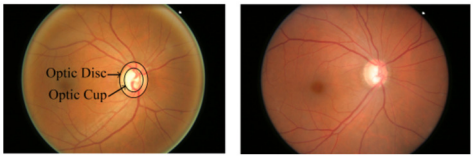

Fig.1: *Sample of fundus images from ORIGA database, left: Normal, right: Glaucoma.*

Clinical tests like Intra-ocular pressure (IOP) measuring technique, testing of the eye visually, optic nerve head (ONH) checking, Tonometry, Pachymetry, and Gonioscopy are the invasive screening methods used for the detection of glaucoma [2]. These treatments need a regular optometrist check-up and other tests for final verification, so the screening process

[1,2,3] The authors are with Department of Electrical Engineering, C. V. Raman Global University, Bhubaneswar, Odisha, India, E-mail: 21080013@cgu-odisha.ac.in, zefree.lazarus@cgu-odisha.ac.in and 20030040@cgu-odisha.ac.in

consumes more time and have high-risk factor due to dilation of the eye and high cost. To alleviate these limitations, non-invasive techniques involving screening methods have already progressed for glaucoma detection. The non-invasive techniques for the automatic detection of glaucoma are based on retinal fundus imaging using a fundus camera.

The retinal fundus imaging process provides a 2D representation of the 3D retinal semi-transparent tissue [3]. A low-power microscope attached to a camera is used for taking fundus images of the interior part of the eye through the pupil. A detailed survey on the fundus photography techniques used for screening various eye diseases and the fundus cameras used (for example Kowa nonmyd7, Kowa VX-10, Canon CF60Uvi, GENESIS D portable, Canon CR6- 45NM, Kowa VX-10a, etc.) can be found at Panwar N. et al. [6]. Nowadays, portable tabletop fundus cameras are being widely used for glaucoma detection. The non-invasive methods of glaucoma detection, such as image processing, machine learning, and deep learning, rely on clinical indicators like the vertical cup-to-disc ratio (CDR), Neuroretinal rim area, ISNT rule [4], rim-to-disc area ratio (RDR), and disc diameter for the detection of glaucoma [5]. Of the mentioned clinical indicators, CDR gained popularity among medical practitioners due to its reliability. Fig. 1 shows the optic disc and optic cup area of a normal fundus image and another glaucomatous image from the ORIGA dataset. The CDR [5] is calculated using the following formula.

$$CDR = \frac{Area\ of\ Optic\ Cup\ (OC)}{Area\ of\ Optic\ Disc\ (OD)} \qquad (1)$$

This study aims to enhance the process of glaucoma detection by introducing a pre-processing step that removes specularities and glares from retinal fundus images. To achieve this, we utilized the popular Robust PCA technique, widely known for its effectiveness in low-level imaging, medical imaging, and 3D computer vision applications [42]. Previous works have also leveraged RPCA for optic disc segmentation, such as Danlei et al.'s proposed low-rank matrix recovery method [9] and Yanwu et al.'s use of a low-rank superpixel method for optic cup segmentation with low-rank representation (LRR) [43]. The longitudinal changes in fundus images have also been successfully detected using low-rank decomposition models [44] and unsupervised sparse representation models [45] with RPCA. Additionally, a patch-based RPCA (P-RPCA) method was proposed by Wenqi Zhu et al. for change detection, specifically in cases of illumination variation [46]. In our study, we utilized RPCA as a pre-processing method to remove specular problems from fundus images and enhance glaucoma detection efficiency. Further details on RPCA and its application in our research are described in section 4.

2. RELATED WORKS

The ultimate aim of this research is the accurate detection of glaucoma; using fundus images. So, in this section, some existing literature related to fundus image quality improvement, segmentation, feature extraction, and image classification methods are described as follows.

Jorg Meier et al. [7] used a fixed configuration of Illumination correction and intensity Inhomogeneity in the pre-processing stage of glaucoma detection. The input image was taken as a product of the illumination component and reflectance components. The inpainting method is used for blood vessel removal from the fundus images and found the region of interest for optic disc segmentation. PCA is used for dimensionality reduction of the input data, and using SVM, the classification accuracy becomes 81Ḣowever, the success rate was less in the case of detecting glaucomatous images than in non-glaucomatous images, and the method showed less reliability for segmentation and feature extraction.

Anusorn et al. [8] used the Intensity-weighted centroid method to find an approximate region of interest (ROI) center. Edge detection and variation level set method are used for OD segmentation and color component analysis method, and threshold level-set method for OC segmentation. The cup-to-disc ratio is calculated by taking a threshold value of 0.65, and the accuracy of detection using this technique is 89%. However, if the eye has peripapillary atrophy, finding the edges of the optic disc can be difficult and in the early stages of glaucoma, it is difficult to calculate CDR using this approach.

For disc vessel removal, morphological operations were performed, and image enhancement was achieved using the Contrast-Limited Adaptive Histogram Equalization (CLAHE) approach [9]. To differentiate the disc from the background, researchers used the Low-Rank Matrix Recovery theory to generate saliency maps. Threshold segmentation is used to create the optic disc, and circular Hough transform divides the disc. The segmentation method has 92.9% accuracy. However, the implementation of this method has not been optimized.

Abhishek Dey et al. [10] proposed a noise reduction and contrast enhancement pre-processing methodology, as well as the Principal Component Analysis (PCA) method for feature extraction and the Support Vector Machine (SVM) method for image classification. For pre-processing and normalization, histogram stretching was performed. With an accuracy of 86%, the k-fold cross-validation approach was used to test the classifier's performance. In this approach, the computational time is more for better results, and positive predictive accuracy is less than negative predictive accuracy.

Soltani et al. [11] proposed an approach to reduce noise from the original ONH images; Gaussian

Table 1: *Summary of Literature for Glaucoma Detection Using Fundus Images.*

Author	Year	Methodology	Features extracted	Data resources	Performance
Jorg Meier et al. [7]	2007	Image Inpainting, PCA, SVM	ONH	200 images from Erlangan Glaucoma Registry (EGR)	Accuracy: 81%
Anusorn et al. [8]	2013	Variation level set, Colour component analysis	CDR	Data collected from Mettapracharak Eye Center	Accuracy: 89%
Danlei Mei et al. [9]	2018	Low-rank matrix recovery, CLAHE	Segmented OD	MESSIDOR	Accuracy: 92.9%
Abhishek Dey et al. [10]	2018	PCA, SVM, Histogram stretching	CDR	Fundus image collected from Susrut Eye Foundation and Research Centre, Kolkata	Accuracy: 86%
Saffarzadeh et al. [12]	2014	K-means clustering, Multi-scale line operator	Blood vessels	STARE, DRIVE	Accuracy: 94.83%, 93.87%
H. Fu et al. [13]	2018	M-Net	CDR	ORIGA, SCES	AUC: 0.85, 0.89
X. Chen et al. [14]	2015	C-CNN	Segmented OD	ORIGA, SCES	AUC: 0.831
Al-Bander et al. [15]	2017	CNN, SVM	Neural features	RIM-ONE	Accuracy: 88.2%
R. Shinde [16]	2021	Le-Net, Brightest Spot Algorithm, U-Net, SVM	CDR	RIM-ONE, DRIVE	Accuracy: 98.67%
Nyul. NG [28]	2009	PCA, SVM, pre-processing processing	Image-based	Erlangan Glaucoma Registry (EGR)	Accuracy: 80%, Provides automatic detection, needs to improve the performance.
Pruthi et al.[29]	2013	Morphological operation, ellipse fitting technique	CDR	20 images from AIIMS, New Delhi	Accuracy: 97.35% using only ten images for testing, CDR calculated, fails to diagnose due to other diseases.
U. Rajendra Acharya et al.[30]	2015	PCA, SVM, NB	Principal components	510 retinal images from Kasturba Medical College, Manipal, India	Accuracy: 93.10%, Gabor transform is used for extracting features, but the method is costly.
Devasia T et al.[31]	2018	Edge detection, Circular Hough Transform	Localized OD	DRIVE, DRIONS, HRF, DIARETDB	Accuracy: 97.27%, Pre-processing consistency needs to be improved.
Mohamed et al.[32]	2019	Superpixel feature extraction, SVM	CDR	RIM-ONE	Accuracy: 98.6%, Features are extracted using superpixel level, but fails to diagnose positive cases.

and Median filters are used. The contours are then detected using the canny detector technique. The Randomized Hough Transform is used to extract features. Finally, to determine patients' conditions, a classification system based on fuzzy logic approach is proposed. The proposed method has a low level of validation, and by using the ISNT rule, many of the glaucomatous cases are diagnosed, so the performance of the fuzzy engine validation was reduced.

For the detection of the retinal vessel network, a pre-processing step based on multi-scale line operators was implemented. The visibility of the vessel was improved, and the impact of bright lesions was minimized using k-means clustering. The retinal vessels were finally discovered in three scales utilizing the line detection operator. The running time of this method is more than other existing methods, and the accuracy is low on the DRIVE database [12].

H. Fu et al. [13] segment the optic disc and cup together, and a multi-label deep network is proposed. The popular feature, called CDR, is then calculated to identify glaucoma disease. The body structure of the proposed M-Net method has a U-shape convolutional network. A multi-scale input layer, U-shape convolutional network, side-output layer, and multi-label loss function are the primary components of the proposed M-Net. The polar transformation is also introduced, which represents the original image in the polar coordinate system for further improvement of segmentation performance. However, abnormal regions and poor contrast quality might readily impact the segmentation accuracy.

Using the outputs of one CNN as the context for the other, a context-based technique [14] for dynamically modifying CNN model learning is proposed, which enhances glaucoma diagnosis. Response normalization layers and overlapping pooling layers are used to reduce overfitting. A CNN was trained and evaluated using a database of 650 cropped images, and the results showed a 0.831 area under the ROC

curve. The most challenging part of implementing CNN is the size of the training dataset, which typically requires many data.

Al. Bander et al. [15] took the resized input images to 227 × 227 pixels, and the input was separated into two categories: 70% used for training and 30% used for validation. The SVM, as a binary classifier, classifies the images as normal or glaucoma after CNN extracts the features from the input images. A convolutional neural network comprises convolutional layers, max-pooling layers, dropout layers, fully connected layers, and activation functions (CNN). A fully connected CNN layer has more parameters, resulting in overfitting and a large amount of training data consumption. In terms of accuracy, sensitivity, and specificity, the approach performed poorly.

R. Shinde [16] proposed an offline CAD system for glaucoma diagnosis. Image processing, deep learning, and machine learning techniques were used to create this application. The bright spot algorithm is used to find regions of interest (ROI), and the LeNet model is preferred to validate the ROI results. U-Net is used to segment the optical disc and optical cups and assemble them using SVM, Neural Network, and Ada Boost. It cannot detect if the same eye has other diseases like diabetes that affect OD segmentation and CDR calculations. The U-Net proves best in OD and OC segmentation, which necessitates using binary pictures as ground truth.

Numerous state-of-the-art methods have been proposed in the literature for glaucoma detection. Neto et al. [37] proposed three criteria for glaucoma classification based on vertical cup-to-disc ratio (vCDR), horizontal cup-to-disc ratio (hCDR), and average cup-to-disc ratio (ACDR) features. Their study found that using vCDR alone produced the best results, achieving a sensitivity of 89% and a precision of 79% using 660 images.

Aurangzeb et al. [38] developed a modified Contrast Limited Adaptive Histogram Equalization (CLAHE) method using Multi-Objective Particle Swarm Optimization (MPSO) in the green channel of fundus images for contrast enhancement. This approach was successfully implemented on the DRIVE and STARE datasets, each containing 40 images, with accuracies of 0.962 and 0.964, respectively.

Wang et al. [39] proposed an image enhancement approach by separating the input image into three layers using total variation. The quality of the images was enhanced by the DIARETDB0 and DIARETDB1 databases, and these images were used for disease detection.

Imtiaz et al. [40] used retinal vessel images for semantic segmentation and glaucoma detection by reducing image size and enhancing contrast. They used the VGG16 convolutional neural network (CNN) for semantic segmentation and achieved an accuracy of 0.993 using the RIM-ONE-r3 dataset by extracting CDR features.

Finally, Bao et al. [41] proposed a self-adaptive transfer learning (SATL) approach for glaucoma classification. This method used the LAG, REFUGE, and a private dataset, but achieved an accuracy of only 0.74.

These state-of-the-art methods represent a range of approaches to glaucoma detection, including feature-based methods, image enhancement techniques, semantic segmentation, and deep learning-based methods. However, there is still room for improvement, particularly in accuracy and robustness.

Table 1 provides an overview of the existing literature on non-invasive techniques for glaucoma detection using retinal fundus imaging.

3. RESEARCH GAP, MOTIVATION, AND OBJECTIVES OF RESEARCH

The technical challenges in the retinal fundus imaging process results in the reduction of the glaucoma detection rate. As there is no internal illumination in the retina, external light is projected into the eye in the fundus imaging process. The small size of the pupil in the eye, the narrow opening in the frontal part, called the iris, and the complexity of the optical system of the eye has always been a naturally challenging factor in fundus imaging [7]. Due to nonuniform illumination, the presence of blood vessels, the geometrical surface of the retina, and dilation of the pupil cause image saturation, specularities, and reflection problem in the fundus images [10]. These speculaities can cause image saturation, low contrast, and changes in color components of anatomical features of the eye, leading to an effect in the screening of glaucoma. Due to these technical challenges in the fundus imaging process, the efficiency of automatic screening methods like cup segmentation, disc segmentation, and calculation of cup-to-disc ratio decreases. The discussion in the related works for glaucoma screening motivates us to adopt the low-rank mathematical algorithm to reduce the artifacts from retinal fundus images.

The proposed methodology combines conventional image processing methods with machine learning to improve glaucoma detection. It consists of three main parts. The first part involves using a low-rank RPCA model to remove specularities caused by nonuniform illumination. We selected the best model among the six approaches for this purpose. The second part focuses on Optic Disc (OD) and Optic Cup (OC) segmentation, achieved using a combination of Canny edge detector and adaptive Thresholding method. Several previous studies have used these methods, such as Zhu et al. [47], who achieved a 92.5% success rate using edge detection with Canny and Sobel methods, and Aquino et al. [48], who used morphological operations and edge detection for OD localization and segmentation with an accuracy of 99%

and 86%, respectively. F. Ghadiri et al. [49] also demonstrated the importance of adaptive Thresholding in edge detection for OD segmentation, with an accuracy of 98% in the KHATAM dataset. Section IV of this manuscript provides further details on the steps for segmentation using the Canny detector and adaptive Thresholding. The result of this step is the extraction of a crucial feature called cup-to-disc Ratio (CDR), which plays a vital role in classifying fundus images. Pranjal et al. [50] proposed a method for glaucoma diagnosis based on CDR and NRR area, achieving an accuracy of 93.85%. Finally, we extract structural features such as OD area, OC area, and CDR, as well as non-structural features [51], such as mean and variance, using the RPCA model. A linear SVM is used for binary classification between normal and abnormal images.

In summary, our proposed model presents an efficient low-rank image pre-processing technique to address the problem of specularities in retinal fundus images, leading to improved feature extraction and better glaucoma detection rates.

The remaining of the article is structured as follows. With a focus on glaucoma screening strategies, section 1 includes the introduction and other applications of RPCA. Some existing methods related to our work and the present state of glaucoma detection models are described in section 2. Section 3 outlined the inspiration behind the current research and its main goals by describing the research problem, motivation, and objectives. The proposed approach is described in section 4. For better understanding, it provides step-by-step outcomes for each module in the proposed approach. The experimental work and results of this research are reported in section 5. This section also includes a description of the datasets utilized for the studies, and a comparison of the five models for glaucoma detection is also shown. The research work's conclusion and potential expansion are described in section 6.

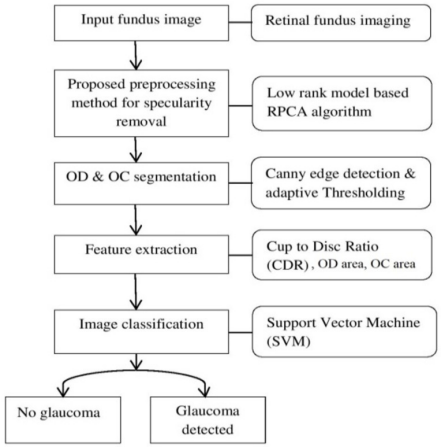

Fig.2: *Proposed architecture for glaucoma detection.*

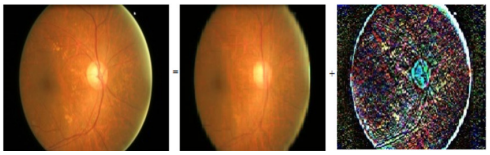

Fig.3: *Left: Corrupted input fundus image, Middle: Low-rank image, and Right: Sparse image.*

4. PROPOSED METHODOLOGY

4.1 Overview of the Methodology

The proposed methodology aims to improve glaucoma detection by removing specularity from retinal fundus images. The end-to-end glaucoma detection approach is depicted in Fig. 2, which comprises four main steps: (1) pre-processing the input retinal fundus image using Robust PCA to remove specularity, (2) segmenting the Optic Disc (OD) and Optic Cup (OC) using Canny edge detection and adaptive Thresholding, (3) extracting the CDR feature, and (4) classifying the image as glaucoma or non-glaucoma using SVM.

To remove specularity from retinal fundus images, Robust PCA is employed in the pre-processing step. The literature [18] suggests that Robust PCA has many low-rank approximation algorithms, and we have selected five algorithms, among which the best one is implemented in our research problem. The OD and OC segmentation is performed using canny edge detection and adaptive Thresholding method. The CDR feature is then extracted from the segmented image, which is used as a base for image classification using SVM. The details of each step in the proposed methodology are explained in the following sections.

4.2 Proposed pre-processing method

In this step, we adopt a low-rank model-based preprocessing algorithm for improving the efficiency of automatic glaucoma detection from retinal fundus images. Candes et al. [18] described Robust PCA by decomposing the specular problems due to non-uniform illumination into a component of low rank (L) and another component of sparse (S) having all the artifacts from the corrupted input image. Mathematically, this problem can be represented as

$$F = L + S \tag{2}$$

where F is the column-wise set of input retinal fundus image data matrix, L and S are the Low-rank matrix and the sparse matrix components. Fig. 3 shows a sample image in which the corrupted input image is decomposed into a low-rank image and a sparse image using the RPCA algorithm. The initial decomposition in robust principal component analysis (RPCA) is described as follows:

$$\min_{L_0,S_0}(rank(L_0)+\gamma||S_0||),\ \text{s.t. } F=L_0+S_0. \quad (3)$$

Where L_0 has a low rank, and S_0 is a sparse matrix, both components are of arbitrary magnitude. The problem of low-rank and sparse decomposition is non-convex and has no effective solution due to the unknown size of both low-rank and sparse matrices. As a result, solving the rank function and l_0-norm-based optimization is often NP-hard [19]. To address this issue, Sobral et al. [20] proposed using low-rank tools, which have since been implemented in various applications. For instance, the RPCA algorithms of the low-rank model have been successfully used for eye detection under spectacles, as shown in the literature by Lazarus et al. [24]. In light of the previous works [18-20], we have considered five algorithms for the pre-processing step, which are listed below:

- Principal Component Pursuit (PCP)
- Accelerated Proximal Gradient (APG)
- Singular Value Thresholding (SVT)
- Augmented Lagrange Multiplier (ALM)
  - Exact Augmented Lagrange Multiplier (EALM)
  - Inexact Augmented Lagrange Multiplier (IALM)

1) Principal Component Pursuit (PCP): E. J. Candes et al. [18] proposed a convex optimization for addressing the robust PCA problem by decomposing into the nuclear norm and the l_1-norm-weighted combination, which is termed Principal Component Pursuit (PCP).

$$\min_{L_0,S_0}(rank||L_0||_*+\gamma||S_0||_1),\ \text{s.t. } F=L_0+S_0. \quad (4)$$

Where γ is called as regularization parameter, and the value of gamma is recommended as $1/\sqrt{\max(r,c)}$.

2) Accelerated Proximal Gradient (APG): Z. Lin et al. [21] proposed a method called the accelerated proximal gradient approach for solving the following underdetermined convex problem.

$$\min_{X\in H}\ s.t.\ F(X)=l(X)+s(X) \quad (5)$$

Where H is the real Hilbert space with the provision of the inner product and a norm. The RPCA decomposition problem in (2) can directly apply to the accelerated proximal gradient approach by identifying: $X=(L,S), l(X)=\frac{1}{\mu}||F-L-S||^2_{F^*}$.

$$l(X)=||L||_*+\gamma||S||_1 \quad (6)$$

Where μ refers to a positive scalar and the value of μ is so adjusted that the decomposition converges a better result.

3) Singular Value Thresholding (SVT): Cai et al. [22] developed the singular value Thresholding algorithm in which the nuclear norm minimization problem can be solved and the solution using SVT by extension problems of the form.

$$\min_{L,S}(||L||_*+||S||_F),\quad s.t.\ A(F)=L+S \quad (7)$$

4) Augmented Lagrange Multiplier (ALM): Z. Lin et al. [21] had given a convex optimization method of the Augmented Lagrange Multiplier approach in which the unconstrained optimization problems can be solved by using:

$$\min\ f(F),\quad s.t.\ h(F)=0 \quad (8)$$

Where F is the objective function of input data and f:$\mathbb{R}^r\to\mathbb{R}$ and h : $\mathbb{R}^c\to\mathbb{R}$.

The method can be defined as the augmented Lagrange function:

$$L(F,Y,\mu)=f(F)+\langle Y,h(F)\rangle+\frac{\mu}{2}||h(F)||_F{}^2 \quad (9)$$

Where Y is the optimal Lagrange multiplier and positive scalar, which is a part of the optimization problem solution through augmented Lagrange multipliers methods.

Applying the low rank and sparse decomposition problem into the ALM method by referencing the following components:

$$\begin{aligned} F=(L,S), f(F)=||L||_*+\gamma||S||_1,\\ h(F)=F-L-S \end{aligned} \quad (10)$$

Then Lagrange function is:

$$\begin{aligned} L(L,S,Y,\mu)=&||L||_*+\gamma||S||_1+\\ &\langle Y,h(F)\rangle+\frac{\mu}{2}||h(F)||_F{}^2 \end{aligned} \quad (11)$$

5) Exact Augmented Lagrange Multiplier (EALM): In Z. Lin et al. [21], the EALM algorithm has excellent convergence property, and the decomposition problem (2) objective function are non-smooth so that it cannot be applied directly. To apply the decomposition problem, the solution statement developed in the following:

$$|(||L_k{}^*||+\gamma||S_k{}^*||_1)-f^*|=O(\mu_{k-1}{}^{-1}) \quad (12)$$

where f^*, depicts the optimal solution to the discussed decomposition problem, μ_K grows iteratively while the EALM approach shows a convergence, Q-linearly, and when μ_K develops faster, the EALM low-rank approximation model will also show a faster convergence.

6) Inexact Augmented Lagrange Multiplier (IALM): Z. Lin et al. [21] described the leading in-

exact ALM (IALM) method because EALM provides a frequent updating of L_K and S_K for solving the sub-problem of the optimal solution of the decomposition problem (2). So, the IALM algorithm provides a better automatic update of L_K and S_K, which can solve the low rank and sparse decomposition problem.

Fewer advancements in EALM results in an inexact ALM approach that provides a convergence almost as quickly as the exact ALM, but with a substantially lower number of practical SVDs. IALM shows a convergence of 5 times faster than APG and has superior accuracy and sensitivity.

4.3 Optic Disc and Optic Cup Segmentation

Segmentation of the optic disc (OD) and optic cup (OC) is a crucial step in detecting glaucoma [34], as the anatomical changes in these regions are strongly correlated with the disease. Detection of ophthalmic diseases relies on changes in shape, area, color, and depth of the OD and OC [35]. The critical feature for glaucoma detection called the cup-to-disc ratio (CDR), can be calculated using the areas of the OD and OC [36].

To locate the boundaries of the OD and OC, we segment the low-rank component of the fundus image that was obtained through the pre-processing step. We separate the red, green, and blue channels of the fundus image, and the green channel provides the strongest contrast, which is useful for edge detection that is then converted into a binary image [9]. Using edge detection, we obtain the disc-shaped structuring element of the OD and OC features by applying Thresholding [8]. In one of our previous works [33], we employed RPCA for OD segmentation, and the results were validated using four classifiers. The preprocessing methods we used included the removal of blood vessels and contrast enhancement via CLAHE, which improved the accuracy of the segmentation of the OD and OC areas.

In this research, the segmentation of OD and OC, a Canny edge detector is used, which includes the following steps.

• **Step 1:** Filtration of the retinal image using a Gaussian filter with a kernel and standard derivative.

$$k(r,c) = \frac{1}{2\pi\sigma^2} \exp\left[-\frac{r^2+c^2}{2\sigma^2}\right] \tag{13}$$

where $k(r,c)$ is a 2D kernel and is the standard derivative.

• **Step 2:** Find the magnitude and orientation of the edge image.

$$g(r,c) = \sqrt{{G_2}^2 + {G_c}^2} \tag{14}$$

$$\alpha(r,c) = \tan^{-1}\sqrt{\frac{{G_c}^2}{{G_r}^2}} \tag{15}$$

where $g(r,c)$ is the gradient amplitude, ${G_r}^2$ and ${G_c}^2$ are the first derivatives in the direction of r and c, and $\alpha(r,c)$ is the gradient angle.

• **Step 3:** Compute the non-maxima suppression by taking the points on the edge that will have high pixel value and others that have zero pixel value.

$$n(r,c) = nms\left[\frac{g(r,c)}{\alpha(r,c)}\right] \tag{16}$$

Where $n(r,c)$ is the output image of non-maxima suppression.

• **Step 4:** Assume two thresholds [8], i.e. high and low; for starting the edge curves, use the high threshold, and to continue them use the low threshold. The gradients above the high threshold are considered edge pixels, and between the low and high thresholds are also related to edge pixels. The gradients below the low threshold are considered non-edge pixels.

4.4 CDR feature extraction

CDR is the most widely used feature for efficient glaucoma detection [7-15]. As shown in Table 1, previous studies have also employed CDR as the fundamental feature for image classification [29] [32]. Therefore, we have used CDR as the primary feature in our research for glaucoma detection. We have calculated the area of segmented OD and OC by employing the centroid localization method to find the circle radius. CDR is then calculated using the formula presented in equation (1).

4.5 Classification using SVM

A supervised learning model called a support vector machine is used to classify the normal fundus image from glaucomatous fundus images. The main concept of SVM is based on separating hyperplane, maximum margin hyperplane, soft margin, and kernel function [23]. A linear SVM can be defined as:

$$f(x) = W^T x + b \tag{17}$$

Our problem is based on binary classification, where the healthy fundus images belong to one class, and glaucomatous images belong to another. In this paper, a linear SVM is used to diagnose the retinal fundus images as healthy or not.

5. EXPERIMENTS AND RESULTS ANALYSIS

In this research, we evaluated the performance of six different RPCA algorithms discussed in section 4 to identify the most effective approach for the preprocessing step of glaucoma detection. Our goal was to find the optimal mathematical solution for this critical step.

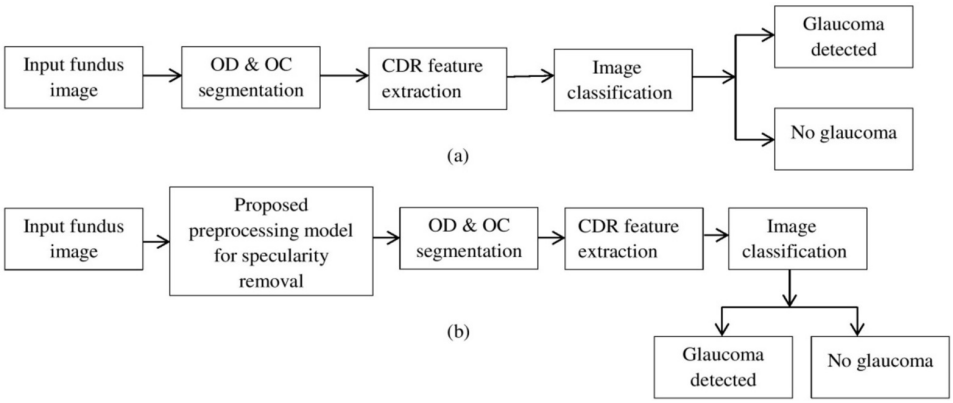

Fig.4: *Block diagram for glaucoma detection (a) Without pre-processing, (b) With pre-processing.*

5.1 The database

For experimental evaluation, the ORIGA database [25] and REFUGE database [26] are used. Drishti-GS-RETINA database [27] is used for the cross-validation method, with 101 retinal fundus images. In the implementation of the proposed model, all retinal fundus images are divided into training (70%) and testing (30%). The details of the database used for experimentation purposes are shown in Table 2.

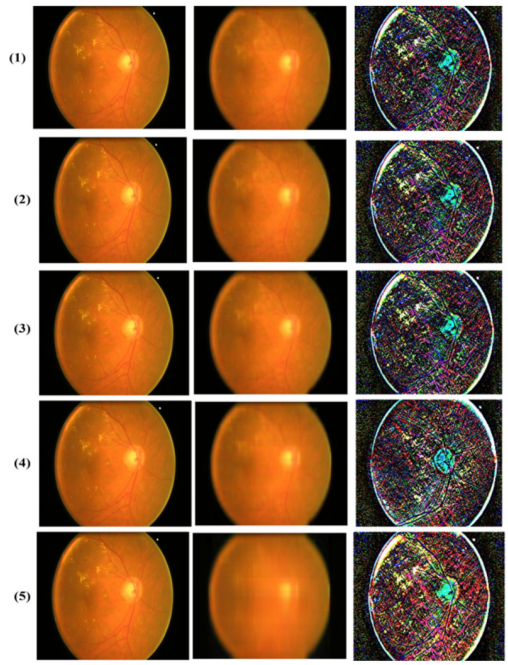

Fig.5: *Decomposed low-rank and sparse images by different approaches of RPCA in five rows (1) IALM (2) EALM (3) APG (4) PCP (5) SVT algorithms. Each row contains the same input fundus image, low-rank, and sparse component images, respectively.*

5.2 Experiment 1

In this experiment, we aim to identify the most efficient RPCA algorithm for our proposed pre-processing step in glaucoma detection. We implemented the six algorithms discussed in Section 4 using MATLAB and evaluated their performance using 650 fundus images from the ORIGA database. We compared the obtained low-rank matrices, which contain the important features of the input data, and the running time of each algorithm. We also calculated the Mean Square Error (MSE) and Peak Signal Noise Ratio (PSNR) between the output image and the ground truth.

We found that the Augmented Lagrange Multiplier (ALM) in the RPCA algorithm was the most effective for our application. It solves the decomposition problem of low-rank and sparse matrices and retains most of the important features of the input data. The low-rank matrix obtained using the IALM algorithm had a rank of 125, which is lower than ELAM's rank of 162 but contains more important features. Additionally, IALM took less time than the other algorithms for removing specularities from the retinal fundus images.

Table 3 summarizes the results of our experiment. We found that IALM provided a maximum PSNR value of 33.47 dB and a minimum MSE value of 29.42. It also converged faster with fewer practical singular value decompositions (SVDs) compared to EALM, which requires more SVDs and is time-consuming.

Fig. 5 shows some examples of the output low-rank and sparse images obtained using IALM, SVT, EALM, APG, and PCP algorithms. The same fundus image from the ORIGA dataset was used as input for all algorithms. It had a specularity problem, and IALM maintained more low-rank information than the other formulations, as seen from the tabular analysis in Table 3. Therefore, we conclude that IALM is the most suitable algorithm for our proposed pre-processing step in glaucoma detection.

5.3 Experiment 2

The ORIGA database contains 168 positive glaucoma images, and those images are used as input for this experiment.

Table 2: *Details of the Database Used.*

Database	Total images	Glaucoma images	Non-glaucoma images	Training images	Testing images
ORIGA	650	168	482	455	195
REFUGE	400	40	360	280	120
DRISTI-GS	101	70	31	71	30

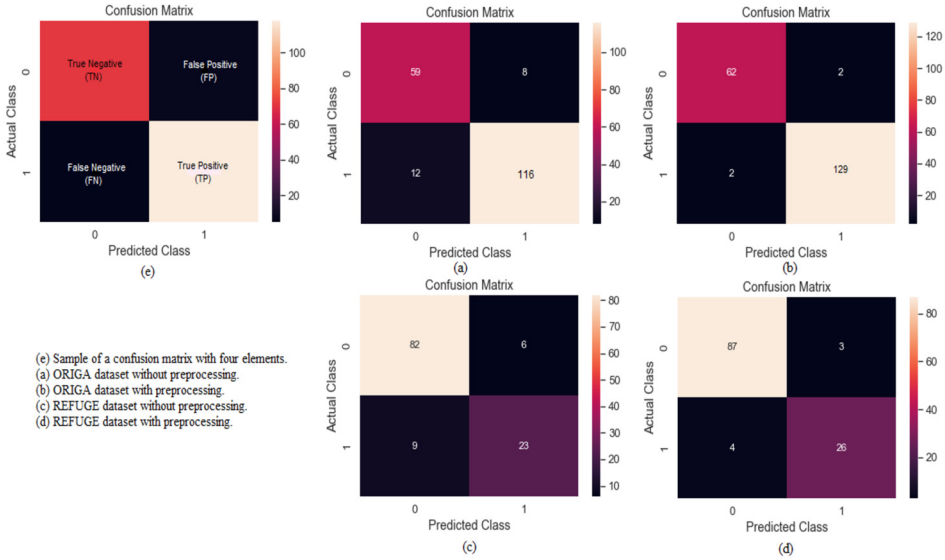

Fig.6: *Confusion matrices obtained after image classification using SVM.*

Table 3: *Comparative Results Conducted on ORIGA Database Showing Rank of input Matrix (F) and Low-Rank Matrix (L).*

Algorithms	Rank of F	Rank of L	Avg. time in sec.	MSE	PSNR in dB
PCP	650	85	434	42.06	31.93
APG	650	137	624	50.38	31.14
SVT	650	72	1820	41.84	31.94
EALM	650	162	754	41.82	31.95
IALM	650	125	162	29.42	33.47

Table 4: *Comparative Results Conducted on ORIGA Database Showing Rank of Input Matrix (F) and Low-Rank Matrix (L) for Three Iterations.*

Algorithms	Rank of F	Rank of L for 3-iterations			Avg. time in
		100	200	300	sec.
IALM	168	14	58	66	0.368
EALM	168	43	64	82	7.17
APG	168	30	59	68	1.72
PCP	168	18	43	54	2.76
SVT	168	12	31	47	34.38

In this experiment, three iterations are taken for each algorithm to evaluate the best low rank at 100, 200, and 300. The operating time taken per image is observed, and the average time is calculated as shown in Table 4. This experiment aims to find an iteration at which the model provides the best low-rank decomposition within less duration of time.

Table 4 shows the variation in the iteration affects the low-rank decomposition, and from all the algorithms, IALM shows the best low-rank decomposition. According to the Table 4 data, by varying no. of iterations, the rank of L is also varied. The IALM algorithm takes 0.368 seconds per image for the low-rank and sparse matrix decomposition, which is the lowest operating time among all.

5.4 Experiment 3

To check the performance of the proposed low-rank model using RPCA, the glaucoma detection experiment is conducted on the ORIGA and REFUGE datasets. From the results of experiments 1 and 2, it is concluded that IALM provides the best low-rank model, which reduces the specularities from the input image and can be used as an image pre-processing step in the glaucoma detection model. So, this experiment is divided into two separate sub-experiments and makes a comparison between the glaucoma detection model without pre-processing shown in Fig. 4(a) and with pre-processing shown in Fig. 4(b). The block diagram shown in Fig. 4(a) provides the experimental idea in a sequence of steps where the input fundus image is directly taken as an input for OD, and OC segmentation. Introducing the proposed pre-processing model before segmentation and other steps are the same, it is described in the block diagram of 4(b).

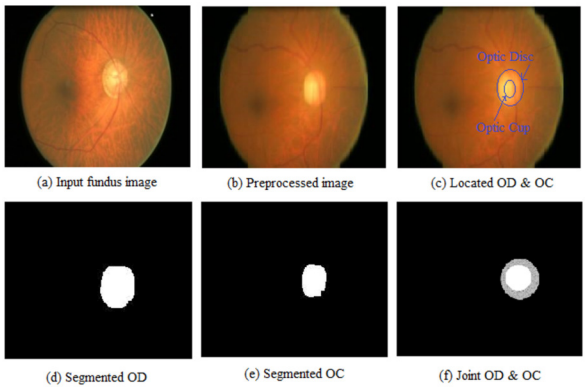

Fig.7: *Top: Input image, After pre-processing and OD and OC segmentation. Bottom: Binary OD, Binary OC, and Ground truth image of joint OD and OC.*

The disc and cup features are extracted using a Canny edge detector, adaptive Thresholding, and centroid localizing method for the calculation of CDR. The extracted CDR features are then applied to the classifier, and based on this feature, SVM classifies glaucoma and non-glaucoma images. If the value of cup to disc ratio is less than 0.45, then it is classified as Non-glaucoma, and if it is greater than 0.45, then glaucoma is detected [2]. The results of image classification and the performance matrices obtained using both the ORIGA and REFUGE datasets are shown in Table 5. The confusion matrices obtained after classification using SVM are shown in Fig. 6.

$$Accuracy = \frac{TP+TN}{TP+TN+FP+FN},\ Precision = \frac{TP}{TP+FP}$$

$$Recall = \frac{TP}{TP+FN},\ F-measure = \frac{2*Recall*Precison}{Recall+Precision}$$

The accuracy increases after adding the proposed pre-processing step in the glaucoma detection model Fig. 4 (b) from 87% to 94% using the REFUGE database and 89% to 97% using the ORIGA database. Table 5 shows the evaluation parameters, and their output values, like precision and recall, also increase in both the databases after using the low-rank model as a pre-processing method. The overall implementation analysis demonstrates that the low-rank decomposition-based pre-processing model for glaucoma detection from fundus images is effective and efficient. Fig. 7 shows the output images at each step of the proposed model with the ground truth from the ORIGA database.

5.5 Experiment 4

In this experiment, the performance of the classifier has been checked by using a stratified cross-validation method. For that purpose, we have taken 101 images from the publically available Drishti-GS-RETINA dataset. Out of 101 retinal fundus images, 71 fundus images were taken to train, and 30 fundus images were taken to validate with three steps. By conducting this experiment, the average accuracy obtained in three steps is calculated. We found that the accuracy of the classifier is 88.13%, and the sensitivity is 79.41%.

Table 5: *Experimental Results Conducted on ORIGA and REFUGE Database.*

Parameters	Database			
	ORIGA		REFUGE	
	Pre-processing		Pre-processing	
	Before	After	Before	After
TP	116	129	23	26
FN	12	2	9	4
TN	59	62	82	87
FP	8	2	6	3
Accuracy	0.89	0.97	0.87	0.94
Precision	0.93	0.98	0.79	0.89
Recall	0.9	0.93	0.71	0.86
F-measure	0.92	0.98	0.75	0.88

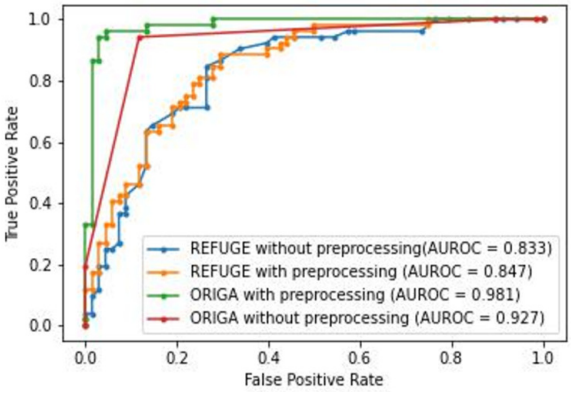

Fig.8: *ROC plotted by comparing the results of Table 5.*

The ROC curves are plotted between the true positive rate and the false positive rate. By taking the output results of the block diagram described in Fig. 4, i.e. with or without the proposed pre-processing step, the area under ROC is calculated as shown in Fig. 8. The maximum AUROC of 0.981 is shown by taking ORIGA dataset with pre-processing and 0.927 of AUROC without pre-processing. Similarly, for the REFUGE dataset, the AUROC of 0.833 and 0.847 are shown in Fig. 8 without and with pre-processing, respectively.

All the implementations were performed with MATLAB R2017a on a PC with Intel (R) Core(TM) i3 - 2130CPU @3.40GHz CPU and 4.00 GB RAM.

6. CONCLUSIONS

This research mainly introduced a low-rank model based on automatic glaucoma detection from fundus images using Robust PCA, which can solve the problems related to the retinal imaging system using a fundus camera. The comparative analysis and implementation of the RPCA algorithm provide low-rank model-based glaucoma detection from retinal fundus images. Among the discussed algorithms, Robust PCA with the IALM algorithm provides the best low-rank decomposition model. The experiments have been done using ORIGA and REFUGE databases containing 650 and 400 fundus retina images, respectively. The success rate of detecting glaucoma increases from 89% to 97% using the ORIGA dataset and from 87% to 94% by using the IALM algorithm and SVM classifier. Using the stratified cross-validation method on the DRISHTI-GS Retinal database, we verified the accuracy of the proposed model, which is 88.13%. The output images after using robust PCA can help doctors to confirm their diagnoses and increases the efficiency of automatic glaucoma detection methods.

The future developments of this study are to enhance the interpretation of the OD and OC segmentation model, including blood vessel removal technique and verification of other clinical indicators using Deep learning techniques to improve the glaucoma detection rate.

References

[1] K. Allison, D. Patel and O. Alabi, "Epidemiology of glaucoma: the past, present, and predictions for the future," *Cureus*, vol. 12, no. 11, e11686, 2020.

[2] D. Bhowmik *et al.*, "Glaucoma-A Eye Disorder Its Causes, Risk Factor, Prevention and Medication," The Pharma Innovation vol. 1, no. 1, Part A, 66, 2012.

[3] M. D. Abràmoff, M. K. Garvin and M. Sonka, "Retinal imaging and image analysis," in *IEEE Reviews in biomedical engineering*, vol. 3, pp. 169-208, 2010.

[4] J. B. Jonas *et al.*, "Ranking of optic disc variables for detection of glaucomatous optic nerve damage," *Investigative Ophthalmology and Visual Science*, vol. 41, no. 7, pp. 1764-1773, 2000.

[5] M. D. H. O. D. , "Optic disc size, an important consideration in the glaucoma evaluation," *Clinical Eye and Vision Care*, vol. 11, no. 2, pp. 59-62, 1999.

[6] N. Panwar, P. Huang, J. Lee, and P.A. Keane, "Fundus photography in the 21st century a review of recent technological advances and their implications for worldwide healthcare," *Telemedicine and e-Health*, vol. 22.3, pp. 198-208, 2016.

[7] J. Meier, R. Bock, G. Michelson and L.G. Nyúl, "Effects of pre-processing eye fundus images on appearance-based glaucoma classification," *Computer Analysis of Images and Patterns: 12th International Conference, CAIP 2007*, Vienna, Austria, August 27-29, Proceedings 12. Springer Berlin Heidelberg, 2007.

[8] C. B. Anusorn *et al.*, "Image processing techniques for glaucoma detection using the cup-to-disc ratio," *Science and Technology Asia*, pp. 22-34, 2013.

[9] D. Mei and D. Chen, "Optic disc segmentation method based on low rank matrix recovery theory," *2018 Chinese Control And Decision Conference (CCDC)*, Shenyang, China, pp. 2626-2630, 2018.

[10] A. Dey and S. K. Bandyopadhyay, "Automated Glaucoma Detection Using Support Vector Machine Classification Method," *British Journal of Medicine and Medical Research*, vol. 11, no. 12, pp. 1-12, 2015.

[11] A. Soltani, T. Battikh, I. Jabri and N. Lakhoua, "A new expert system based on fuzzy logic and image processing algorithms for early glaucoma diagnosis," *Biomedical Signal Processing and Control*, vol. 40, pp. 366-377, 2018.

[12] V. M. Saffarzadeh, A. Osareh and B. Shadgar, "Vessel segmentation in retinal images using multi-scale line operator and K-means clustering," *Journal of Medical signals and sensors*, vol. 4, no. 2, pp. 122-129, 2014.

[13] H. Fu *et al.*, "Joint optic disc and cup segmentation based on multi-label deep network and polar transformation," *IEEE Transactions on medical imaging*, vol. 37, no. 7, pp. 1597-1605, 2018.

[14] X. Chen *et al.*, "Automatic feature learning for glaucoma detection based on deep learning," *Medical Image Computing and ComputerAssisted InterventionMICCAI 2015: 18th International Conference*, Munich, Germany, October 5-9, 2015, Proceedings, Part III 18. Springer International Publishing, 2015.

[15] B. Al-Bander, W. Al-Nuaimy, M. A. Al-Taee and Y. Zheng, "Automated glaucoma diagnosis using deep learning approach," *2017 14th International Multi-Conference on Systems, Signals & Devices (SSD)*, Marrakech, Morocco, pp. 207-210, 2017.

[16] R. Shinde, "Glaucoma detection in retinal fundus images using U-Net and supervised machine learning algorithms," *Intelligence-Based Medicine*, vol. 5, 100038, 2021.

[17] K. Kim, "Face Recognition using Principal Component Analysis," University of Maryland, College Park, MD 20742, USA.

[18] E. J. Candès *et al.*, "Robust principal component analysis?," *Journal of the ACM (JACM)*, vol. 58, no.3, pp. 1-37, 2011.

[19] J. Wright *et al.*, "Robust principal component analysis: Exact recovery of corrupted low-rank matrices via convex optimization," *Advances in neural information processing systems*, vol. 22, 2009.

[20] A. Sobral, T. Bouwmans and E. Zahzah, "Lrslibrary: Low-rank and sparse tools for background modeling and subtraction in videos," *Robust Low-Rank and Sparse Matrix Decomposition: Applications in Image and Video Processing*, pp. 14(1-15), 2016.

[21] Z. Lin, M. Chen and Y. Ma, "The augmented lagrange multiplier method for exact recovery of corrupted low-rank matrices," *arXiv preprint arXiv*:1009.5055, 2010.

[22] J. F. Cai, EJ Candès, and Z. Shen, "A singular value thresholding algorithm for matrix completion," *SIAM Journal on optimization*, vol. 20.4, pp. 1956-1982, 2010.

[23] W. S. Noble, "What is a support vector machine?," *Nature biotechnology*, vol. 24.12, pp. 1565-1567, 2006.

[24] M. Z. Lazarus and S. Gupta, "A low rank model based improved eye detection under spectacles," *2016 IEEE 7th Annual Ubiquitous Computing, Electronics & Mobile Communication Conference (UEMCON)*, New York, NY, USA, pp. 1-6, 2016.

[25] Z. Zhang *et al.*, "ORIGA-light: An online retinal fundus image database for glaucoma analysis and research," *2010 Annual International Conference of the IEEE Engineering in Medicine and Biology*, Buenos Aires, Argentina, pp. 3065-3068, 2010.

[26] J. I. Orlando *et al.*, "Refuge challenge: A unified framework for evaluating automated methods for glaucoma assessment from fundus photographs," *Medical image analysis*, vol. 59, 101570, 2020.

[27] J. Sivaswamy, S. R. Krishnadas, G. Datt Joshi, M. Jain and A. U. Syed Tabish, "DrishtiGS: Retinal image dataset for optic nerve head(ONH) segmentation," *2014 IEEE 11th International Symposium on Biomedical Imaging (ISBI)*, Beijing, China, pp. 53-56, 2014.

[28] L. G. Nyl, "Retinal image analysis for automated glaucoma risk evaluation," *MIPPR 2009: Medical Imaging, Parallel Processing of Images, and Optimization Techniques*, vol. 7497. SPIE, 2009.

[29] J. Pruthi and S. Mukherjee, "Computer-based early diagnosis of glaucoma in biomedical data using image processing and automated early nerve fiber layer defects detection using feature extraction in retinal colored stereo fundus images," *International Journal of Scientific and Engineering Research*, vol. 4.4, pp. 1822-28, 2013.

[30] U. R. Acharya *et al.*, "Decision support system for glaucoma using Gabor transformation," *Biomedical Signal Processing and Control*, vol. 15 pp. 18-26, 2015.

[31] T. Devasia, P. Jacob, T. Thomas, "Automatic optic disc localization in color retinal fundus images," *Adv. Comput. Sci. Technol*, vol. 11, no.1, pp. 1-13, 2018.

[32] N. A. Mohamed, M. A. Zulkifley, W. M. D. W. Zaki and A. Hussain, "An automated glaucoma screening system using cup-to-disc ratio via simple linear iterative clustering superpixel approach," *Biomedical Signal Processing and Control*, vol. 53, 101454, 2019.

[33] S. Lenka and M. Z. Lazarus, "Optic Disc Segmentation using Non-convex Rank Approximation from Retinal Fundus Images," *2022 IEEE 2nd International Symposium on Sustainable Energy, Signal Processing and Cyber Security (iSSSC)*, Gunupur, Odisha, India, pp. 1-6, 2022.

[34] M. T. Nicolela and J. R. Vianna, "Optic nerve: clinical examination," *Pearls of Glaucoma Management*, pp. 17-26, 2016.

[35] H. Li and O. Chutatape, "A Model-Based Approach for Automated Feature Extraction in Fundus Images," *ICCV.*, vol. 2003. 2003.

[36] J. Cheng *et al.*, "Superpixel classification based optic disc and optic cup segmentation for glaucoma screening," in *IEEE Transactions on Medical Imaging*, vol. 32, no. 6, pp. 1019-1032, June 2013.

[37] A. Neto *et al.*, "Optic disc and cup segmentations for glaucoma assessment using cup-to-disc ratio," *Procedia Computer Science*, vol. 196, pp. 485-492, 2022.

[38] K. Aurangzeb, S. Aslam, M. Alhussein, R. A. Naqvi, M. Arsalan and S. I. Haider, "Contrast Enhancement of Fundus Images by Employing Modified PSO for Improving the Performance of Deep Learning Models," in *IEEE Access*, vol. 9, pp. 47930-47945, 2021.

[39] J. Wang, Y. J. Li, and K. F. Yang, "Retinal fundus image enhancement with image decomposition and visual adaptation," *Computers in Biology and Medicine*, vol. 128, 104116, 2021.

[40] R. Imtiaz *et al.*, "Screening of Glaucoma disease from retinal vessel images using semantic segmentation," *Computers and Electrical Engineering*, Vol. 91, 107036, 2021.

[41] Y. Bao *et al.*, "Self-adaptive Transfer Learning for Multicenter Glaucoma Classification in Fundus Retina Images," *Ophthalmic Medical Image Analysis: 8th International Workshop, OMIA 2021*, Held in Conjunction with MICCAI 2021, Strasbourg, France, September 27, 2021, Proceedings 8. Springer International Publishing, 2021.

[42] T. Bouwmans, S. Javed, H. Zhang, Z. Lin and R. Otazo, "On the Applications of Robust PCA in Image and Video Processing," in *Proceedings*

of the IEEE, vol. 106, no. 8, pp. 1427-1457, Aug. 2018.

[43] Y. Xu *et al.*, "Optic cup segmentation for glaucoma detection using low-rank superpixel representation," *Medical Image Computing and Computer-Assisted Intervention MICCAI 2014: 17th International Conference*, Boston, MA, USA, September 14-18, 2014, Proceedings, Part I 17. Springer International Publishing, 2014.

[44] Y. Fu *et al.*, "Automatic detection of longitudinal changes for retinal fundus images based on low-rank decomposition," *Journal of Medical Imaging and Health Informatics*, vol. 8, no.2, pp. 284-294, 2018.

[45] Y. Fu *et al.*, "Change detection based on unsupervised sparse representation for fundus image pair," *Scientific Reports*, vol. 12, no. 1, pp.1- 14, 2022.

[46] W. Zhu *et al.*, "Changed Detection Based on Patch Robust Principal Component Analysis," *Applied Sciences*, vol. 12, no.15, 7713, 2022.

[47] X. Zhu and R. M. Rangayyan, "Detection of the optic disc in images of the retina using the Hough transform," *2008 30th annual International Conference of the IEEE Engineering in Medicine and Biology Society*, pp. 3546-3549, 2008.

[48] A. Aquino, M. E. Gegúndez-Arias and D. Marín, "Detecting the optic disc boundary in digital fundus images using morphological, edge detection, and feature extraction techniques," *IEEE Transactions on Medical Imaging*, vol. 29.11, pp. 1860-1869, 2010.

[49] F. Ghadiri, R. Bergevin and M. Shafiee, "An adaptive thresholding approach for automatic optic disk segmentation," *arXiv preprint arXiv*, 1710.05104, 2017.

[50] P. Das, S. R. Nirmala and J. P. Medhi, "Diagnosis of glaucoma using CDR and NRR area in retina images," *Network Modeling Analysis in Health Informatics and Bioinformatics*, vol. 5, pp. 1-14, 2016.

[51] A. A. Salam *et al.*, "Automated detection of glaucoma using structural and non-structural features," *Springer Plus*, vol. 5, pp. 1-21, 2016.

Satyabrata Lenka is a diligent researcher who has completed his B.Tech and M.Tech degrees in Electrical Engineering from Biju Patnaik University of Technology, Odisha, India, in 2015 and 2020, respectively. Currently pursuing his Ph.D. (Tech.) from C.V. Raman Global University, Odisha, India, Satyabrata focuses his research on areas such as Biomedical Signal Processing, Power Electronics, and Renewable Energy. With a strong foundation in electrical engineering and a drive for innovation, he strives to make significant contributions to these fields.

Mayaluri Zefree Lazarus is a highly accomplished professional with a strong background in electrical and electronic engineering. He obtained his B.Tech in EEE from the esteemed University College of Engineering (Kakatiya University) in 2008. Building upon this foundation, he went on to complete his M.Tech in ECE (Digital Systems and Computer Electronics) in 2011. In 2021, he successfully earned his Ph.D. from the department of Electrical Engineering at NIT Rourkela, specializing in Digital Image Processing.

Currently holding the position of Assistant Professor in the Department of Electrical Engineering at C.V. Raman Global University, M.Z. Lazarus also serves as the Deputy Dean for International Relations. His research interests encompass computer vision, inverse problems, digital image processing, and biomedical image processing.

Saubhagya Ranjan Behera is an expert in Mechatronics Engineering, specializing in PLC, SCADA, IoT, and Industry 4.0. Possessing a Postgraduate degree in Mechatronics Engineering, he boasts a comprehensive understanding of this interdisciplinary domain. As an enthusiastic educator, Saubhagya Ranjan Behera imparts valuable knowledge and skills to students and professionals alike through engaging lectures and practical demonstrations. His research primarily focuses on computer vision and machine learning, contributing to the advancements in these areas. With a passion for both teaching and research, he continuously strives to bridge the gap between academia and industry.